The crystal structure of quenselite*

By ROLAND C. ROUSE

Ann Arbor, Michigan

Auszug

Quenselit, $PbMnO_2OH$, hat die Gitterkonstanten $a = 5,61$ Å, $b = 5,70$ Å, $c = 9,15$ Å, $\beta = 93,0°$, die Raumgruppe $P2/a$; $Z = 4$. Die von BYSTRÖM gefundene Raumgruppe und Struktur erwiesen sich als unrichtig. Die Atomlagen wurden bis zu $10,6\%$ verfeinert. Die Struktur baut sich aus vier Schichten ebener dichtester Kugelpackung parallel (001) auf. Zwei benachbarte Schichten sind nur von O-Ionen, die beiden anderen von OH-Gruppen und in nur angenäherten Lagen von Pb-Ionen besetzt. Die beiden Sauerstoffschichten werden durch die dazwischenliegenden Mn-Ionen zu einer brucitähnlichen Schicht aus deformierten MnO_6-Oktaedern verbunden. Die beiden anderen Schichten bestehen aus endlosen Ketten von $PbO(OH)_3$-Pyramiden ähnlich wie beim gelben PbO. Ein System schwacher Wasserstoff-Bindungen zwischen den Ketten und den brucitartigen Schichten wird erläutert.

Abstract

Quenselite, $PbMnO_2OH$, is monoclinic, $P2/a$, with $a = 5.61$, $b = 5.70$, $c = 9.15$ Å, and $\beta = 93.0°$; $Z = 4$. The structure and space group proposed by BYSTRÖM are not correct. The correct structure, which has been refined to an R value of 10.6%, consists of four hexagonal closest-packed oxygen layers stacked normal to [001] with Pb^{+2} ions nearly occupying anion sites. Brucite-type layers parallel to (001) are composed of distorted MnO_6 octahedra characteristic of the Jahn-Teller effect. Sandwiched between these are infinite chains of $PbO(OH)_3$ pyramids resembling those in yellow PbO. A system of weak hydrogen bonds linking the chains and the brucite-type layers is proposed.

Introduction

A structure for the mineral quenselite, $PbMnO_2OH$, was proposed by BYSTRÖM (1945). Using Weissenberg and powder photographs, he determined the unit cell to be monoclinic, $P2_1/c$, with $a = 9.118$,

$b = 5.676$, $c = 5.604$ Å, and $\beta = 87.0°$. There are four formula weights per cell. Using visually estimated intensities from Weissenberg photographs, he deduced a structure which consists of alternating layers of anions and cations parallel to (100). The layer sequence is Mn—O—Pb—OH—Pb—O—Mn with Mn octahedrally coordinated by O (brucite-type layer) and Pb coordinated by $4\,OH + 2\,O$. Considering the three shortest lead-oxygen distances, Pb is situated at the apex of a distorted trigonal pyramid. This structure is consistent with the perfect cleavage along {100}. Unfortunately, the symmetry of the structure appeared to be $P2$ and Byström was unable to derive this or any other reasonable structure in the true space group, $P2_1/c$.

Quenselite was restudied by Nuffield, but the only published record of this is a brief reference in *The Peacock atlas of x-ray powder data* (Berry and Thompson, 1962). Nuffield reoriented the unit cell, the transformation being:

$$
\begin{array}{ccc}
\text{Nuffield} & & \text{Byström} \\
a & = & -c \\
b & = & b \\
c & = & a
\end{array}
$$

The unit cell parameters are given as $a = 5.61$, $b = 5.68$, $c = 9.16$ Å, $\beta = 93° 18'$ with space group $C2/m$. In the present study the setting of Nuffield has been used.

The author has re-examined the crystal structure of quenselite using crystals from Långban, Sweden, kindly provided by Dr. J. A. Mandarino of the Royal Ontario Museum (specimen # M 14607). Weissenberg and precession photographs using $CuK\alpha$ and $MoK\alpha$ radiation confirmed the monoclinic symmetry. Unit-cell parameters are $a = 5.61$, $b = 5.70$, $c = 9.15$ Å, and $\beta = 93.0°$. The magnitudes of a, b, and c were obtained from Bradley-Jay extrapolations of single-crystal diffractometer data using $MoK\alpha$ radiation. The space group is $P2/a$, which agrees with Byström's finding except for the absence of the 2_1 screw axis. A very pronounced substructure is present, whose symmetry conforms to the space group $C2/m$. Possibly Nuffield's photographs were underexposed, in which case only the intense substructure reflections would appear, falsely indicating space group $C2/m$. Inspection of the structure shows that the false C-centered effect results from the C-centered arrangement of the Pb atoms.

Refinement of the structure

Using a prismatic crystal of size $0.03 \times 0.03 \times 0.17$ mm and the equi-inclination Weissenberg method, a total of 811 intensities were measured on an automated single-crystal diffractometer. Monochromated $MoK\alpha$ radiation and pulse-height analysis were employed. The data were corrected for Lorentz, polarization, and absorption effects and symmetrically redundant reflections were removed. With the resulting 691 reflections and Byström's atom coordinates, transformed as noted above, refinement of the structure was begun in space group $P2$. The refinement was carried out by the method of least squares using the IBM 360 program SFLSQ5 written by Dr. C. T. Prewitt. Scattering factors for Pb^+ were obtained from Cromer and Waber (1965) and those for $Mn^{+3/2}$ and O^- from the *International tables for x-ray crystallography* (1962). Anomalous dispersion corrections for Pb and Mn taken from Cromer (1965) were applied throughout the refinement. All unobserved reflections were assigned estimated values for I_{obs} according to the equation of Prewitt and Burnham (1966). These unobserved reflections were included in the calculation of the R value but were rejected in the refinement if $|F|_{calc} < |F|_{min}$ as recommended by Dunning and Vand (1969). All reflections were equally weighted.

After several least-squares cycles in which atomic coordinates and isotropic temperature factors were varied, the refinement converged to a conventional R value of 10.7%. All refined parameters were reasonable except for the OH temperature factors which had become very large. At this point a difference Fourier synthesis was computed; it revealed that Byström had incorrectly placed the four OH groups. This is not surprising considering that he had located the anions on spatial and crystal-chemical grounds alone. Refining the correct OH coordinates as obtained from the difference map produced no change in the R value, however. The rather high value of 10.7% is due to the fact that half of all reflections are weak or unobserved superstructure reflections, the latter being represented by estimated values. The R value, excluding unobserved reflections, is 5.5%.

At this point an attempt was made to resolve the discrepancy between the apparent symmetry of the structure, $P2$, and the true symmetry, $P2/a$. A reconsideration of the structure showed that the atom coordinates could be fitted to the equipoints of $P2/a$ simply by adding $3/4$ to x and y. This corresponds to shifting the origin of the structure onto an inversion center in $P2/a$. Further refinement in the

Table 1. *Structure factors*

h	k	l	F_o	F_c
0	2	0	178.7	175.7
		3	25.0	25.5
		4	74.2	70.5
		5	22.2	17.6
		6	93.2	88.0
		7	9.7	4.3
0	2	1	98.9	96.5
		3	9.0	7.8
		4	115.1	110.8
		5	9.0	2.6
		6	42.7	43.2
		7	9.6	9.3
0	1	2	6.4	2.5
		2	73.8	70.2
		3	7.6	0.6
		4	90.4	86.0
		5	9.1	1.7
		6	30.9	32.8
		7	9.8	9.7
0	0	3	198.5	217.8
		1	7.0	10.5
		2	154.3	153.4
		3	22.2	20.3
		4	93.9	89.7
		5	9.2	14.0
		6	89.0	85.7
		7	10.0	4.4
0	0	4	101.7	96.9
		1	7.2	9.7
		2	103.2	101.6
		3	8.0	10.1
		4	89.0	87.0
		5	9.0	5.6
		6	47.0	46.1
		7	10.1	9.0
0	0	5	8.5	11.0
		1	7.8	1.0
		2	42.3	38.2
		3	8.3	4.1
		4	51.8	50.4
		5	9.0	0.4
		6	18.9	19.4
0	0	6	160.5	161.0
		1	8.4	0.9
		2	118.1	115.6
		3	8.5	9.4
		4	73.8	71.1
		5	9.2	12.9
		6	74.5	73.4
0	0	7	62.8	57.6
		1	8.8	8.0
		2	90.8	87.5
		3	8.8	8.2
		4	94.8	94.8
		5	9.3	3.3
		6	51.8	47.5
0	0	8	26.1	32.0
		1	9.0	0.8
		2	9.2	13.1
		3	9.3	5.1
		4	50.0	44.8
		5	9.7	3.1
0	0	9	124.9	121.1
		1	9.0	0.4
		2	81.7	81.0
		3	9.7	5.8
		4	44.7	43.3
		5	9.8	9.7
0	0	10	51.9	46.9
		1	9.2	1.6
		2	74.0	70.1
		3	9.9	1.9
		4	80.7	80.1
0	0	11	22.2	22.7
		1	9.5	2.9
		2	9.0	0.4
		3	10.0	6.1
0	0	12	74.2	67.7
		1	9.8	0.5
1	2	0	26.1	23.8
		3	7.8	4.8
		4	8.6	7.8
		5	8.8	7.9
		6	9.2	16.9
		7	9.6	5.8
1	2	1	52.2	54.7
		-1	34.9	28.0
1	3	1	133.9	128.6
		-1	118.6	116.9
1	4	1	8.6	5.5
		-1	9.0	9.4
1	5	1	93.2	87.2
		-1	96.7	94.3
1	6	1	9.1	13.1
		-1	27.4	25.5
1	7	1	62.1	60.4
		-1	61.3	62.3
1	1	2	139.6	140.2
		-2	145.7	152.1
1	2	2	74.8	69.6
1	2	-2	21.9	21.8
1	3	2	130.2	121.4
		-2	135.3	135.8
1	4	2	9.0	8.1
		-2	8.6	2.4
1	5	2	101.2	99.5
		-2	97.9	96.1
1	6	2	39.3	41.2
		-2	9.3	2.7
1	7	2	69.4	68.5
		-2	63.9	65.6
1	1	3	6.6	5.2
		-3	36.6	33.0
1	2	3	61.7	57.3
		-3	37.7	37.6
1	3	3	15.8	17.7
		-3	31.0	23.0
1	4	3	21.0	5.0
		-3	8.6	5.4
1	5	3	9.2	8.7
		-3	28.3	23.8
1	6	3	29.4	28.0
		-3	27.1	22.2
1	7	3	9.7	3.1
		-3	26.2	17.6
1	1	4	124.3	125.8
		-4	105.6	104.4
1	2	4	65.2	64.8
		-4	55.3	51.3
1	3	4	105.1	101.8
		-4	91.6	87.4
1	4	4	8.7	7.7
		-4	8.6	7.4
1	5	4	72.7	68.1
		-4	75.8	74.3
1	6	4	23.3	20.0
		-4	32.7	34.1
1	7	4	48.9	48.8
		-4	54.2	53.4
1	1	5	125.9	126.0
		-5	131.3	129.5
1	2	5	33.5	35.5
		-5	48.6	51.2
1	3	5	111.4	109.2
		-5	121.9	121.7
1	4	5	8.6	10.4
		-5	16.5	4.1
1	5	5	94.4	90.3
		-5	87.8	88.9
1	6	5	33.0	31.4
		-5	22.6	16.2
1	1	6	26.6	25.6
		-6	34.9	37.1
1	2	6	26.9	20.1
		-6	51.7	50.4
1	3	6	30.7	27.3
		-6	37.5	35.9
1	4	6	8.7	4.0
		-6	8.7	2.4
1	5	6	16.2	18.4
		-6	40.6	36.1
1	6	6	9.9	11.2
		-6	32.0	31.1
1	1	7	84.3	85.7
		-7	65.5	67.8
1	2	7	18.3	26.0
		-7	37.7	33.0
1	3	7	68.9	69.2
		-7	65.3	60.4
1	4	7	8.8	4.8
		-7	8.9	6.9
1	5	7	51.7	47.5
		-7	53.0	52.9
1	6	7	24.4	6.3
		-7	24.5	27.2
1	1	8	109.8	102.7
		-8	104.0	104.8
1	2	8	9.0	11.2
		-8	26.4	25.5
1	3	8	88.1	86.9
		-8	97.4	93.0
1	4	8	9.0	11.2
		-8	9.3	3.6
1	5	8	72.8	72.4
		-8	73.8	70.5
1	1	9	38.7	32.2
		-9	42.5	38.8
1	2	9	9.4	21.0
		-9	16.7	18.7
1	3	9	36.2	33.2
		-9	50.1	40.2
1	4	9	23.8	1.0
		-9	18.0	3.7
1	5	9	45.2	38.7
		-9	55.5	50.8
1	1	10	46.8	42.7
		-10	31.3	30.4
1	2	10	9.2	9.9
		-10	50.2	45.6
1	3	10	37.8	35.1
1	4	10	9.9	3.7
		-10	26.5	7.0
1	1	11	78.9	76.8
		-11	76.9	74.7
1	2	11	24.3	20.8
		-11	9.7	18.5
1	3	11	68.5	63.5
		-11	70.4	70.3
1	1	-12	42.8	39.6
2	2	0	156.1	155.4
		3	17.4	10.1
		4	144.1	142.7
		5	8.8	7.7
		6	81.8	78.7
		7	9.6	14.1
2	2	1	64.3	66.5
		-1	91.6	92.5
2	3	1	23.3	14.4
		-1	8.3	4.4
2	4	1	31.4	26.8
		-1	39.0	38.5
2	5	1	8.8	8.1
		-1	9.1	11.6
2	6	1	37.9	38.3
		-1	55.1	57.6
2	7	1	9.5	2.3
		-1	24.2	4.4
2	1	2	6.6	5.4
2	2	2	70.2	68.7
		-2	46.7	47.6
2	3	2	8.1	1.1
		-2	8.1	13.5
2	4	2	45.7	45.3
		-2	9.0	14.9
2	5	2	9.0	7.4
		-2	9.2	8.6
2	6	2	53.6	50.0
		-2	25.8	24.5
2	7	2	9.7	3.7
		-2	23.4	3.7
2	0	3	120.8	119.2
		-3	96.8	93.1
2	1	3	6.8	1.9
		-3	7.1	9.8
2	2	3	144.0	140.1
		-3	137.2	140.4
2	3	3	8.2	2.9
		-3	8.1	10.5
2	4	3	138.2	132.1
		-3	139.7	144.5
2	5	3	9.1	8.1
		-3	9.2	7.0
2	6	3	74.8	76.8
		-3	71.9	73.1
2	7	3	9.9	16.0
		-3	24.4	12.9
2	0	4	124.8	127.3
		-4	155.6	162.7
2	1	4	7.5	2.9
		-4	7.6	5.2
2	2	4	77.4	73.1
		-4	98.0	97.9
2	3	4	22.4	10.4
		-4	17.0	13.2
2	4	4	16.6	28.8
		-4	39.4	44.0
2	5	4	9.4	9.1
		-4	8.9	10.2
2	6	4	42.6	45.0
		-4	54.8	59.1
2	0	5	93.6	92.7
		-5	58.4	60.7
2	1	5	16.5	4.9
		-5	8.4	4.8
2	2	5	46.3	43.5
		-5	22.1	20.2
2	3	5	8.4	0.8
		-5	8.6	9.5
2	4	5	8.7	9.2
		-5	8.7	9.7
2	5	5	9.1	7.2
		-5	9.1	3.2
2	6	5	40.0	33.1
		-5	9.7	14.0
2	0	6	70.5	65.2
		-6	100.9	99.4
2	1	6	8.7	0.9
		-6	8.7	5.6
2	2	6	111.3	109.1
		-6	111.7	109.8
2	3	6	8.6	1.3
		-6	8.5	7.8
2	4	6	129.4	126.8
		-6	99.9	99.4
2	5	6	9.0	5.0
		-6	8.9	7.7
2	6	6	75.5	68.3
		-6	62.1	58.4
2	0	7	114.0	112.4
		-7	116.8	117.2
2	1	7	18.5	0.3
		-7	8.8	4.1
2	2	7	66.2	67.9
		-7	86.7	86.8
2	3	7	18.6	6.1
		-7	17.2	11.4
2	4	7	29.7	29.5
		-7	57.1	55.2
2	5	7	9.7	8.7
		-7	9.4	9.4
2	0	8	51.2	50.6
		-8	16.6	22.7
2	1	8	9.2	0.9
		-8	8.8	2.8
2	2	8	27.3	21.4
		-8	9.4	0.4
2	3	8	9.0	2.4
		-8	9.2	0.2
2	4	8	9.3	3.4
		-8	9.5	14.4
2	5	8	9.7	3.8
		-8	9.8	3.2
2	0	9	67.0	62.2
		-9	60.2	56.0
2	1	9	9.0	1.0
		-9	8.9	6.2
2	2	9	85.8	80.0
		-9	74.3	76.4
2	3	9	20.7	1.7
		-9	9.7	6.9
2	4	9	92.2	84.9
		-9	78.1	81.6
2	0	10	75.7	72.9
		-10	105.3	107.0
2	1	10	9.4	0.3
		-10	9.1	1.3
2	2	10	61.9	56.5
		-10	69.0	71.0
2	3	10	10.0	3.6
		-10	10.0	7.9
2	4	-10	29.1	35.2
2	0	11	24.3	21.4
		-11	9.4	16.5
2	1	11	22.6	0.1
		-11	9.6	2.8
2	2	11	10.0	6.3
		-11	21.4	10.0
3	2	0	64.5	64.3
		3	26.3	22.2
		4	8.7	3.5
		5	8.9	7.3
		6	40.2	28.1
3	2	1	49.0	42.4
		-1	44.5	46.2
3	3	1	106.5	105.3
		-1	90.9	91.4
3	4	1	8.8	13.6
		-1	9.0	3.1
3	5	1	82.3	84.4
		-1	67.7	64.3
3	6	1	42.1	36.5
		-1	9.4	15.5
3	1	2	113.4	115.2
		2	53.3	50.7
3	2	2	20.3	24.3
		2	101.1	100.0
3	3	2	108.6	114.0
		-2	8.8	6.0
3	4	2	8.9	13.2
		-2	65.5	69.7
3	5	2	91.6	91.8
		-2	9.4	16.0
3	6	2	28.2	27.6
3	1	3	7.6	8.1
		-3	52.3	51.4
3	2	3	34.5	35.1
		-3	32.1	30.1
3	3	3	8.3	5.2
		-3	38.5	35.3
3	4	3	8.9	0.9
		-3	8.5	2.2
3	5	3	9.4	3.2
		-3	23.1	19.4
3	6	3	22.0	18.6
		-3	26.0	11.6
3	1	4	110.0	111.3
		-4	73.9	75.2
3	2	4	24.6	9.9
		-4	23.4	16.6
3	3	4	91.7	88.4
		-4	68.9	72.6
3	4	4	8.7	13.8
		-4	8.5	1.6
3	5	4	75.2	70.9
		-4	53.4	53.8
3	6	4	21.2	19.6
		-4	9.9	4.4
3	1	5	106.4	109.0
		-5	115.7	118.3
3	2	5	23.2	26.1

Table 1. *(Continued)*

h	k	l	F_o	F_c	h	k	l	F_o	F_c	h	k	l	F_o	F_c	h	k	l	F_o	F_c
3	2	-5	15.9	20.9	4	5	-2	9.5	2.9	4	4	-8	9.9	6.4	5	3	-7	26.6	28.0
3	3	5	93.0	90.6			-2	9.7	1.3	4	6	9	86.7	86.7	5	1	8	65.8	64.3
		-5	97.5	100.3	4	6	2	31.9	41.9			-9	76.5	79.2			-8	66.3	72.6
3	4	5	24.6	6.1			-2	9.8	8.4	4	1	9	9.7	0.0			-8	10.2	19.0
		-5	8.8	10.4	4	0	3	144.0	153.7			-9	9.5	3.7	5	2	8	19.6	21.6
3	5	5	62.4	64.6			-3	136.9	145.1	4	2	9	71.0	67.1			-8	66.6	70.0
		-5	78.7	84.1	4	1	3	8.1	2.0			-9	53.8	58.3	5	3	-8	47.4	49.4
3	6	5	9.9	4.1			-3	8.1	1.8	4	3	-9	10.3	9.1	6	2	0	77.4	78.3
		-5	9.9	24.6	4	2	3	103.0	104.7	4	0	10	27.7	25.9			3	9.4	1.8
3	1	6	8.9	11.8			-3	98.8	101.4			-10	57.2	55.1			4	91.7	92.8
		-6	48.9	49.5	4	3	3	8.5	5.0	4	1	-10	9.6	3.7	6	2	1	8.9	16.5
3	2	6	27.4	19.4			-3	8.4	6.1	4	2	-10	60.7	65.8			-1	58.8	65.1
		-6	33.9	34.0	4	4	3	59.5	59.9	5	2	0	32.8	26.5	6	3	1	20.5	0.5
3	3	6	8.7	9.1			-3	56.4	60.0			3	21.6	22.4			-1	9.8	7.2
		-6	45.4	47.2	4	5	3	9.6	11.8			4	9.3	4.8	6	4	1	10.3	9.4
3	4	6	8.9	4.0			-3	9.4	12.6			5	16.8	22.1			-1	32.2	37.8
		-6	8.7	2.0	4	6	3	69.1	71.3	5	2	1	28.8	28.6			2	89.2	91.5
3	5	6	9.4	11.5			-3	64.3	67.0			-1	30.3	29.3	6	1	2	8.5	0.3
		-6	25.8	31.5	4	0	4	8.9	9.2	5	3	1	86.0	88.9	6	2	2	50.4	56.2
3	1	7	84.8	77.8			-4	52.3	47.4			-1	53.8	55.4			-2	26.8	4.7
		-7	46.1	47.3	4	1	4	8.3	0.6	5	4	1	9.6	6.3	6	3	2	20.0	5.7
3	2	7	8.9	19.6			-4	8.6	2.4			-1	9.4	8.1			-2	16.9	2.6
		-7	23.1	32.0	4	2	4	40.6	47.5	5	5	1	65.8	64.6			2	22.5	23.4
3	3	7	64.4	64.2			-4	84.6	86.0			-1	45.6	47.6			2	10.1	7.9
		-7	50.2	51.0	4	3	4	8.6	2.3	5	1	2	75.3	79.3	6	0	3	55.5	56.3
3	4	7	8.9	9.1			-4	8.6	1.2	5	2	2	8.5	8.4			-3	58.5	57.2
		-7	19.8	0.8	4	4	4	72.8	72.7			-2	39.2	45.8	6	1	3	26.0	3.0
3	5	7	51.5	54.4			-4	100.4	103.7	5	3	2	64.4	64.5			3	8.8	0.8
		-7	37.6	37.8	4	5	4	10.1	0.8			-2	85.4	91.2	6	2	3	77.4	77.3
3	1	8	91.9	88.6			-4	17.5	2.7	5	4	2	9.6	10.8			-3	65.1	71.6
		-8	84.9	89.8	4	6	4	57.0	53.8			-2	9.6	8.3	6	3	3	9.5	3.1
3	2	8	38.5	36.8	4	0	4	22.8	17.6	5	5	2	55.9	53.3			-3	17.6	1.6
		-8	33.5	32.8			-5	27.2	30.4			-2	61.0	65.0	6	4	3	85.5	85.6
3	3	8	79.6	77.2	4	1	5	8.5	2.4	5	1	3	8.3	10.3			-3	70.6	74.7
		-8	79.9	81.4			-5	9.0	4.6			-3	43.9	42.7	6	0	4	40.0	42.4
3	4	8	9.5	6.8	4	2	5	47.3	48.4	5	2	3	20.8	18.0			-4	78.0	85.2
		-8	9.5	6.2			-5	8.7	7.8			-3	28.9	27.8	6	1	4	9.3	2.5
3	5	-8	70.8	72.2	4	3	5	8.5	0.9	5	3	3	8.8	12.2			-4	9.2	1.8
3	1	9	31.5	22.6			-5	8.6	2.3			-3	28.4	35.3	6	2	4	25.1	24.8
		-9	49.4	48.7	4	4	5	66.0	65.5	5	4	3	9.5	2.0			-4	63.6	66.0
3	2	9	26.8	26.2			-5	29.9	32.2			-3	9.2	6.3	6	3	4	9.5	0.6
		-9	28.0	29.0	4	5	5	9.9	1.0	5	5	3	17.6	15.2			-4	9.4	2.6
3	3	9	9.7	15.7			-5	27.4	2.7			-3	24.6	31.8	6	4	-4	41.7	42.2
		-9	45.0	44.5	4	0	6	114.9	115.7	5	1	4	81.7	86.9	6	0	5	60.9	60.2
3	4	-9	9.8	1.7			-6	118.4	125.2			-4	47.3	48.1			-5	17.7	15.7
3	1	10	52.7	48.4	4	1	6	19.0	0.9	5	2	4	18.3	25.3	6	1	5	9.6	2.4
		-10	28.4	31.1			-6	9.3	4.2			-4	20.6	23.3			-5	26.8	2.6
3	2	10	32.4	23.2	4	2	6	87.8	87.5	5	3	4	75.1	75.3	6	2	5	38.0	41.6
		-10	20.8	20.8			-6	79.9	82.0			-4	42.4	45.9			-5	9.6	5.8
3	3	-10	33.3	26.4	4	3	6	15.8	4.8	5	4	4	9.4	4.4	6	3	5	9.5	7.0
3	1	-11	65.6	63.2			-6	8.9	11.2			-4	9.1	5.5			-5	19.9	0.2
4	2	0	111.6	109.6	4	4	6	56.0	59.0	5	5	-4	40.4	41.8	6	0	6	55.5	58.7
		3	8.8	6.7			-6	38.4	40.9	5	1	5	72.1	75.0			-6	31.8	35.1
		4	74.6	78.4	4	5	6	9.8	9.7			-5	94.3	97.3	6	1	6	10.1	1.8
		5	9.2	10.3			-6	9.7	9.0	5	2	5	9.0	19.8			-6	10.0	3.3
		6	72.2	74.9	4	0	7	36.5	32.1			-5	19.0	24.8	6	2	6	68.3	68.5
4	2	1	43.9	40.2			-7	54.8	56.4	5	3	5	64.1	63.3			-6	54.7	57.7
		-1	80.5	83.8	4	1	7	9.4	0.9			-5	75.4	80.6	6	3	-6	9.8	2.6
4	3	1	8.8	2.0			-7	20.3	0.8	5	4	5	20.3	8.8	6	0	-7	78.2	89.0
		-1	8.8	2.7	4	2	7	47.7	49.3			-5	9.5	5.9	6	1	-7	10.2	2.5
4	4	1	50.9	53.2			-7	76.2	78.8	5	1	6	9.5	3.6	6	2	-7	59.1	61.1
		-1	87.4	87.0	4	3	7	9.2	2.5			-6	45.5	49.1	7	2	0	10.1	11.0
4	5	1	18.8	1.5			-7	9.4	1.2	5	2	6	28.9	32.1	7	1	1	63.0	67.9
		-1	9.4	4.3	4	4	7	56.3	56.9			-6	9.2	8.9	7	2	1	9.6	12.1
4	6	1	9.7	20.5			-7	84.0	86.7	5	3	6	84.0	86.7			1	10.3	18.2
		-1	47.8	49.7	4	0	8	27.4	18.0			-6	40.4	40.7	7	1	2	51.3	50.8
4	1	2	7.8	1.4			-8	21.9	22.8	5	4	6	9.5	0.7	7	2	2	35.7	22.4
4	2	2	70.2	68.4	4	1	8	9.5	2.0			-6	21.7	8.1			-2	16.7	13.5
		-2	26.3	25.7			-8	9.2	0.1	5	1	7	72.3	62.8	7	1	3	20.7	16.5
4	3	2	8.6	3.4	4	2	8	25.3	29.8			-7	29.6	31.6			-3	32.4	34.4
		-2	8.5	3.9			-8	9.6	5.3	5	2	7	22.0	28.9	7	2	-3	22.6	23.0
4	4	2	86.4	86.8	4	3	8	9.5	1.5			-7	17.2	15.8	7	1	-4	31.7	31.5
		-2	37.4	35.3			-8	9.8	1.7	5	3	7	62.4	60.0					

Table 2

Refined atom parameters of quenselite (standard errors in parentheses)

Atom		x	y	z	B
Pb	$4g$	− 0.0092 (2)	0.2464 (3)	0.3410 (1)	0.90 (2)
Mn(1)	$2e$	3/4	0.8725 (12)	0	0.40 (9)
Mn(2)	$2e$	3/4	0.3856 (12)	0	0.40 (9)
O(1)	$4g$	0.1121 (37)	0.3740 (37)	0.8788 (20)	0.28 (28)
O(2)	$4g$	0.9039 (41)	0.1322 (41)	0.1127 (22)	0.69 (31)
OH	$4g$	0.9044 (41)	0.1531 (42)	0.6289 (23)	0.96 (32)

Table 3. *Interatomic distances and angles*
(standard errors in parentheses)

Pb—O(2)	2.22 (2) Å		Pb—Pb	3.972 (3) Å	(2×)
OH	2.31 (2)		Pb	4.006 (2)	
OH	2.37 (2)		Pb	4.031 (2)	(2×)
OH	2.76 (2)		Pb	4.043 (3)	
O(1)	2.99 (2)		Pb	4.074 (2)	
O(1)	3.16 (2)		Pb	4.101 (3)	
Mean	2.63 Å				
Pb—O(1)	4.38 (2) Å				
Pb—O(1)	4.99 (2)				

Mn(1)—O(1)	1.93 (2) Å	(2×)	Mn(2)—O(1)	1.90 (2) Å	(2×)
O(2)	1.98 (2)	(2×)	O(2)	1.95 (2)	(2×)
O(2)	2.25 (2)	(2×)	O(1)	2.37 (2)	(2×)
Mean	2.05 Å		Mean	2.07 Å	

O(1)—O(1)	2.64 (4) Å		O(2)—O(2)	2.62 (4) Å	
OH	2.81 (3)		O(2)	2.82 (4)	
O(2)	2.82 (3)		OH	3.00 (3)	
O(2)	2.85 (2)		OH	3.02 (3)	
O(2)	2.89 (3)		O(2)	3.19 (2)	(2×)
O(1)	2.98 (4)				
O(2)	3.04 (3)		OH—OH	2.85 (4) Å	
O(1)	3.15 (2)	(2×)	OH	3.17 (4)	
O(2)	3.21 (3)		OH	3.31 (3)	(2×)

O(2)—Pb—OH	83.1 (8)°		OH—Pb—O(1)	147.2 (6)°
O(2)—Pb—OH	82.4 (8)		OH—Pb—OH	76.0 (8)
O(2)—Pb—OH	143.4 (7)		OH—Pb—O(1)	144.4 (6)
O(2)—Pb—O(1)	63.5 (7)		OH—Pb—O(1)	96.7 (6)
O(2)—Pb—O(1)	66.2 (7)		OH—Pb—O(1)	138.2 (6)
OH—Pb—OH	89.9 (6)		OH—Pb—O(1)	144.8 (6)
OH—Pb—OH	67.9 (9)		O(1)—Pb—O(1)	61.6 (4)
OH—Pb—O(1)	95.4 (7)			

O(1)—Mn(1)—O(1)	86.3 (12)°		O(1)—Mn(2)—O(1)	87.8 (13)°
O(1)—Mn(1)—O(2)	95.4 (8)		O(1)—Mn(2)—O(2)	95.0 (8)
O(1)—Mn(1)—O(2)	176.1 (9)		O(1)—Mn(2)—O(2)	176.0 (9)
O(1)—Mn(1)—O(2)	85.7 (8)		O(1)—Mn(2)—O(1)	87.7 (8)
O(1)—Mn(1)—O(2)	93.3 (8)		O(1)—Mn(2)—O(1)	94.6 (8)
O(2)—Mn(1)—O(2)	83.0 (14)		O(2)—Mn(2)—O(2)	84.4 (14)
O(2)—Mn(1)—O(2)	83.3 (9)		O(2)—Mn(2)—O(1)	81.9 (8)
O(2)—Mn(1)—O(2)	97.7 (8)		O(2)—Mn(2)—O(1)	95.7 (8)
O(2)—Mn(1)—O(2)	178.6 (14)		O(1)—Mn(2)—O(1)	176.8 (10)

centrosymmetric space group produced no significant change in the
R value but did reduce the standard deviations of the atom parameters.
The final R values are 10.6⁰/₀ for all reflections and 5.0⁰/₀ excluding the
unobserved ones. Structure factors are listed in Table 1 and refined
atom parameters in Table 2. Table 3 contains interatomic distances
and angles calculated by the program ORFFE (Busing, Martin and
Levy, 1964) utilizing the least-squares variance-covariance matrix.

Structure and bonding

Although only four atoms were incorrectly placed by Byström,
these four OH play a critical role in the structure. It is clear from Fig. 1
that the layer sequence is Mn—O—(Pb,OH)—(OH,Pb)—O—Mn not
Mn—O—Pb—OH—Pb—O—Mn. The OH are separated into two layers
and are nearly coplanar with Pb. In fact, if the Pb atoms are shifted by
~ 0.9 Å they and the OH groups form somewhat distorted closest-
packed layers (Fig. 2). Thus, the structure of quenselite is based upon
four closest-packed Pb plus anion layers. This is confirmed by the c
parameter, 9.15 Å, which is very nearly four times the height of a
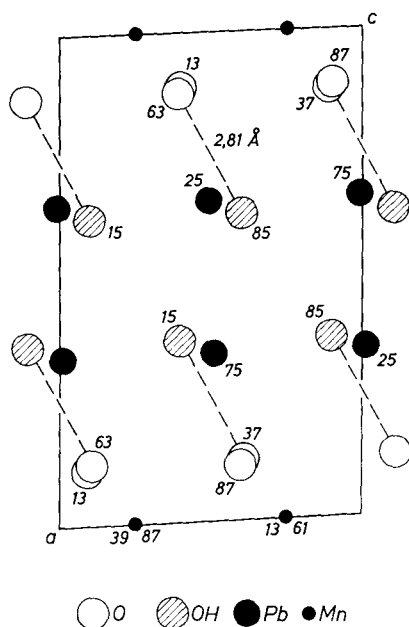
Fig.1. Projection of the quenselite structure on (010) showing proposed hydrogen
bonds as dashed lines. Numbers are y coordinates in hundredths
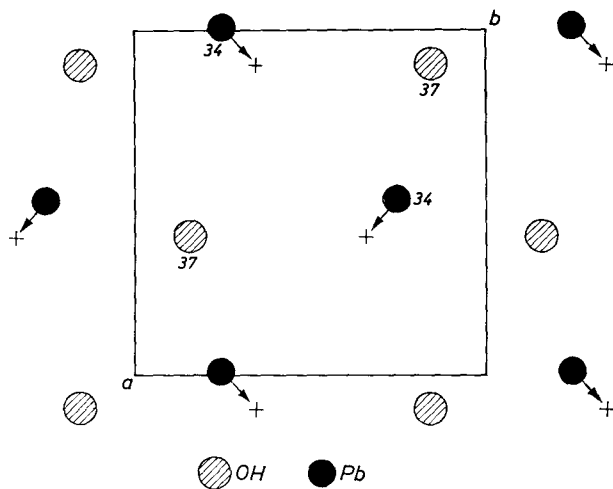
Fig.2. One (Pb + OH) layer showing the shifts necessary to place Pb on an anion site. Numerals indicate z coordinates in hundredths
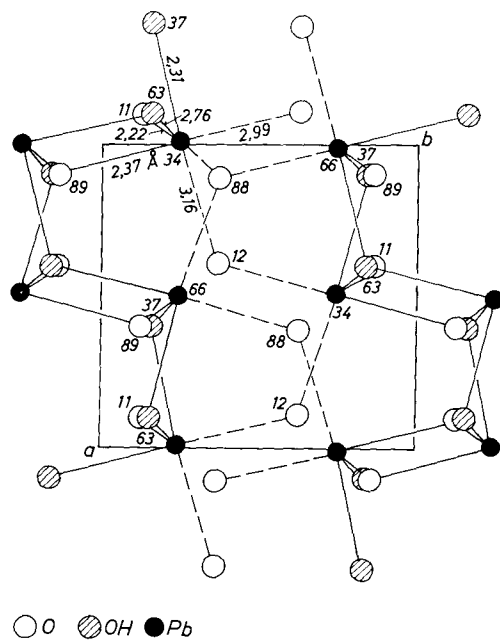
Fig.3. Projection on (001) showing the PbO(OH)₃ chains. Numerals give z coordinates in hundredths

closest-packed oxygen layer (4 × 2.29 = 9.16 Å). The stacking sequence is *ABAB* ..., i.e. hexagonal closest-packing. Using the average of a and b ($a' = 5.65$ Å), the ratio c/a' is 1.62, close to the ideal value of 1.633 for hexagonal closest-packing.

The structural role of Pb in quenselite is not entirely equivalent to that of an anion, however. A Pb^{+2} ion (radius ~ 1.2 Å) cannot occupy an anion site in a closest-packed oxygen framework without fitting poorly. In addition, occupying an anion site would place each Pb in contact with four other Pb, greatly increasing repulsions between cations. On the other hand, Pb^{+2} cannot fit into an octahedral void (ideal radius = 0.58 Å) without great distortion of the oxygen framework. Thus, a compromise is effected with Pb assuming an irregular six-fold coordination with O and OH.

Considering only its four nearest anion neighbors, Pb lies at the apex of a distorted square pyramid (Fig. 3). The same configuration occurs in yellow PbO (KAY, 1961), red PbO (LECIEJEWICZ, 1961), and other Pb^{+2} compounds; it suggests a degree of directed or covalent bonding between lead and oxygen (DICKENS, 1965a,b). The shortest Pb—O distance in quenselite is 2.22 Å compared to 2.21 Å in yellow PbO. DICKENS (1965a) has shown that Pb—O bonds in the latter compound must have a high degree of covalency. Considering all six anion neighbors, however, the average distance is 2.63 Å, which is close to the 2.58 Å predicted for an ionic bond (SHANNON and PREWITT, 1969). In red PbO (DICKENS, 1965b) the PbO_4 square pyramid is regular and the unshared electron pair on the Pb is localized in an sp hybrid orbital directed away from the plane of the four oxygen atoms. If such were the case in quenselite, the lone pair would be directed toward two distant oxygen atoms at 2.99 and 3.16 Å, and toward two more distant oxygen atoms at 4.38 and 4.99 Å, completing a highly distorted cubic coordination around the Pb atom. These four very long lead-oxygen distances are explainable in terms of repulsion between the lone pair and the oxygen anions.

Another analogy to the Pb oxides is the presence of infinite, zigzag, $PbO(OH)_3$ chains parallel to (010), which are similar to those in yellow PbO. In both forms of PbO interlayer bonds consist of weak van der Waals forces between the lone pairs on the Pb atoms. Reference to Fig. 3 shows that, in quenselite, Pb atoms lie adjacent to one another in adjacent chains. The Pb—Pb separation (3.972 Å) is close to that in red PbO (3.88 Å). Thus, separate PbO-type chains in quenselite appear to be linked in the b direction by: (1) shared oxygen atoms at $z = 0.88$

and $z = 0.12$, and (2) van der Waals bonds between pairs of Pb atoms across the center of the unit cell.

The Mn ions lie in distorted oxygen octahedra, which share edges to form a brucite-type layer parallel to (001) (Fig. 4). These octahedra exhibit the elongation along one axis commonly found in Mn^{+3} coordination polyhedra distorted by the Jahn-Teller effect. However, the average Mn—O distances, 2.05 and 2.07 Å, are both very close to the average value of 2.045 Å predicted by SHANNON and PREWITT (1969). The apparent presence of Jahn-Teller distortions is the most cogent argument for the presence of Mn^{+3} rather than a mixture of Mn^{+2} and Mn^{+4}.
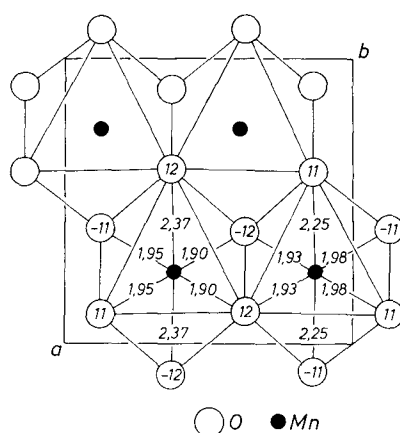
Fig.4. Projection on (001) showing the brucite-type layer of distorted octahedra. Numerals give z coordinates in hundredths

To investigate the possibility of hydrogen bonding and verify the position of the OH groups, a calculation of the electrostatic bond strength delivered to each anion was made. Using the model of DONNAY and ALLMANN (1970), the sums of the bond strengths to O(1), O(2), and OH are 1.84, 2.16, and 1.30, respectively. Assuming hydrogen bonds between the four O(1) and the four OH, these become 2.00, 2.16, and 1.14. Clearly, this is a more reasonable charge distribution. Further support for this assumption is the 2.81 Å distance between O(1) and OH. Excluding shared octahedron edges, this is the shortest anion-anion separation in the structure.

The (Pb + OH) layers and the brucite-type MnO_6 layers thus appear to be bonded together by: (1) certain mainly weak electrostatic attractions between Pb and O, and (2) a system of weak hydrogen

bonds between O(1) and OH. This placement of the hydrogen bonds leaves only van der Waals forces to bridge the gap between the two OH layers (Fig. 1). Such weak interlayer bonding readily explains the perfect {001} cleavage of quenselite.

Related structures

The significance of the quenselite structure lies in its role as a connecting link between certain of the Pb oxides and the lithiophorite-chalcophanite group (STRUNZ, 1970). In addition to red and yellow PbO, quenselite has structural similarities to Pb_2O_3 (BOUVAIST and WEIGEL, 1970). The marked similarity in type and sequence of layers is well shown in (010) projections of the two structures.

Lithiophorite, $(Al,Li)MnO_2(OH)_2$, (WADSLEY, 1952) is monoclinic, $C2/m$, with $a = 5.06$, $b = 2.91$, $c = 9.55$ Å, and $\beta = 100°\ 30'$. Like quenselite it contains brucite-type layers parallel to (001) with an anion-cation layer sequence Mn—O—OH—(Al,Li)—OH—O—Mn. Unlike quenselite it contains no large cations but does have an extra OH. This means there are no anion vacancies in the closest-packed layers and no large cations to fill them. In both minerals the O and OH layers appear to be linked by weak hydrogen bonds.

Chalcophanite, ideally $ZnMn_3O_7 \cdot 3H_2O$, (WADSLEY, 1955) is triclinic but pseudomonoclinic, $C2/m$. The structure is composed of a series of layers Mn—O—Zn—H_2O—Zn—O—Mn parallel to (001). The MnO_6 layers are again of the brucite type, but the octahedral Zn layers are only partially filled. There are also hydrogen bonds between O and H_2O across the Zn layer.

Crednerite, $CuMnO_2$, (KONDRASHEV, 1958) is also monoclinic, $C2/m$, with $a = 5.58$, $b = 2.88$, $c = 5.88$ Å and $\beta = 104°\ 00'$. The structure consists of two MnO_6 layers parallel to (001) with the oxygen atoms of adjacent layers forming trigonal prisms. Two-coordinated Cu^{+1} atoms occupy the midpoints of the vertical edges of these prisms. The layer sequence is Mn—O—Cu—O—Mn. As in quenselite the distortion of the octahedra indicates Mn^{+3}.

Acknowledgements

References

L. G. BERRY and R. M. THOMPSON (1962), X-ray powder data for ore minerals. The Peacock Atlas. Geol. Soc. Amer., Mem. 85.

J. BOUVAIST et D. WEIGEL (1970), Sesquioxyde de plomb, Pb_2O_3. I. Détermination de la structure. Acta Crystallogr. A **26**, 501—510.

W. R. BUSING, K. O. MARTIN and H. A. LEVY (1964), ORFFE, a Fortran crystallographic function and error program. U. S. Atomic Energy Commission Publication, ORNL-TM-306.

A. BYSTRÖM (1945), The structure of quenselite, $PbMnO_2OH$. Arkiv Kemi, Min., Geol. **19A**, No. 35.

D. T. CROMER (1965), Anomalous dispersion corrections computed from self-consistent field relativistic Dirac-Slater wave functions. Acta Crystallogr. **18**, 17—23.

D. T. CROMER and J. T. WABER (1965), Scattering factors computed from relativistic Dirac-Slater wave functions. Acta Crystallogr. **18**, 104—109.

B. DICKENS (1965a), The bonding in the yellow form of lead monoxide. J. Inorg. Nucl. Chem. **27**, 1495—1501.

B. DICKENS (1965b), The bonding in red PbO. J. Inorg. Nucl. Chem. **27**, 1503—1507.

G. DONNAY and R. ALLMANN (1970), How to recognize O^{2-}, OH^-, and H_2O in crystal structures determined by x-rays. Amer. Mineral. **55**, 1003—1015.

A. J. DUNNING and V. VAND (1969), Treatment of accidentally absent reflexions in least-squares refinement of crystal structures. Acta Crystallogr. A **25**, 489—491.

International tables for x-ray crystallography (1962), Kynoch Press, Birmingham, **3**, 202.

M. I. KAY (1961), A neutron diffraction study of orthorhombic PbO. Acta Crystallogr. **14**, 80—81.

IU. D. KONDRASHEV (1958), The crystal structure and composition of crednerite, $CuMnO_2$. Soviet Physics—Crystallogr. **3**, 703—706.

J. LECIEJEWICZ (1961), On the crystal structure of tetragonal (red) PbO. Acta Crystallogr. **14**, 1304.

C. T. PREWITT and C. W. BURNHAM (1966), The crystal structure of jadeite. Amer. Mineral. **51**, 956—975.

R. D. SHANNON and C. T. PREWITT (1969), Effective ionic radii in oxides and fluorides. Acta Crystallogr. B **25**, 925—946.

H. STRUNZ (1970), *Mineralogische Tabellen*. Akademische Verlagsgesellschaft, Leipzig.

A. D. WADSLEY (1952), The structure of lithiophorite, $(Al,Li)MnO_2(OH)_2$. Acta Crystallogr. **5**, 676—680.

A. D. WADSLEY (1955), The crystal structure of chalcophanite, $ZnMn_3O_7 \cdot 3H_2O$. Acta Crystallogr. **8**, 165—172.